

RESEARCH LETTER

10.1002/2016GL068457

Key Points:

- Mars' south polar cap contains a deposit with enough CO₂ to double the atmospheric pressure if it sublimated
- Surface and radar observations show this deposit to be three CO₂ subunits capped by water ice
- Modeling allows us to constrain the minimum age of this deposit to be ~300 kyr old

Supporting Information:

- Supporting Information S1
- Text S1–S2
- Figure S1
- Figure S2
- Figure S3
- Figure S4
- Figure S5

Correspondence to:

C. J. Bierson,
cthomas1@ucsc.edu

Citation:

Bierson, C. J., R. J. Phillips, I. B. Smith, S. E. Wood, N. E. Putzig, D. Nunes, and S. Byrne (2016), Stratigraphy and evolution of the buried CO₂ deposit in the Martian south polar cap, *Geophys. Res. Lett.*, *43*, 4172–4179, doi:10.1002/2016GL068457.

Received 29 FEB 2016

Accepted 22 APR 2016

Accepted article online 25 MAY 2016

Published online 10 MAY 2016

Stratigraphy and evolution of the buried CO₂ deposit in the Martian south polar cap

C. J. Bierson¹, R. J. Phillips^{2,3}, I. B. Smith⁴, S. E. Wood⁵, N. E. Putzig⁴, D. Nunes⁶, and S. Byrne⁷

¹Department of Earth and Planetary Sciences, University of California, Santa Cruz, California, USA, ²Planetary Science Directorate, Southwest Research Institute, Boulder, Colorado, USA, ³McDonnell Center for the Space Sciences and Department of Earth and Planetary Sciences, Washington University, St. Louis, Missouri, USA, ⁴Department of Space Studies, Southwest Research Institute, Boulder, Colorado, USA, ⁵Department of Earth and Space Sciences, University of Washington, Seattle, Washington, USA, ⁶California Institute of Technology, Jet Propulsion Laboratory, Pasadena, California, USA, ⁷Lunar and Planetary Lab, University of Arizona, Tucson, Arizona, USA

Abstract Observations by the Shallow Radar instrument on Mars Reconnaissance Orbiter reveal several deposits of buried CO₂ ice within the south polar layered deposits. Here we present mapping that demonstrates this unit is 18% larger than previously estimated, containing enough mass to double the atmospheric pressure on Mars if sublimated. We find three distinct subunits of CO₂ ice, each capped by a thin (10–60 m) bounding layer (BL). Multiple lines of evidence suggest that each BL is dominated by water ice. We model the history of CO₂ accumulation at the poles based on obliquity and insolation variability during the last 1 Myr assuming a total mass budget consisting of the current atmosphere and the sequestered ice. Our model predicts that CO₂ ice has accumulated over large areas several times during that period, in agreement with the radar findings of multiple periods of accumulation.

1. Introduction

Obliquity and orbital parameters strongly force the insolation and thus stability of both CO₂ and water ices at different latitudes on Mars [Murray *et al.*, 1973; Ward, 1973, 1974; Laskar *et al.*, 2002, 2004; Manning *et al.*, 2006; Levrard *et al.*, 2007]. In the current epoch, surface water ice is most stable at the poles, and there is strong evidence that water cycles between midlatitudes at high obliquity and the poles at low obliquity [Kreslavsky and Head, 2002; Head *et al.*, 2003; Madeleine *et al.*, 2009].

Carbon dioxide ice is less stable at the surface of Mars than water ice and undergoes strong seasonal cycles of deposition and sublimation. These seasonal cycles drive the transport of large quantities of CO₂ between the north and south poles each year, which in turn has a strong seasonal effect on the surface pressure of the thin atmosphere (~600 ± 100 Pa) [Hess *et al.*, 1979, 1980; Tillman *et al.*, 1993].

Longer cycles also exist for CO₂ deposits at the South Pole. The South Pole Residual Cap (SPRC) is a several meters thick veneer composed primarily of CO₂ ice. Recent work has shown that the SPRC is sublimating in some places and accumulating in others [Thomas *et al.*, 2013, 2016; Becerra *et al.*, 2015], with a possible cycle time for the residual CO₂ cap of about 100 years [Byrne *et al.*, 2014]. Corresponding to even longer cycles, CO₂ ice is found in reservoirs other than the atmosphere and thin surface deposits. Using Shallow Radar (SHARAD) instrument data [Seu *et al.*, 2007] from the Mars Reconnaissance Orbiter (MRO), Phillips *et al.* [2011] mapped a massive deposit of buried CO₂ ice within the south polar layered deposits (SPLD) in a radar stratigraphic unit called “reflection-free zone three” (RFZ₃). They measured volumes that if sublimated would increase the surface pressure of Mars by 65–85% (400 to 500 Pa). Their results support climate models that predicted partial atmospheric collapse on the poles over cycles of the planet's obliquity [Ward *et al.*, 1974; Toon *et al.*, 1980; François *et al.*, 1990; Jakosky *et al.*, 1995; Forget, 1998; Armstrong *et al.*, 2004; Manning *et al.*, 2006; Wood *et al.*, 2012].

1.1. Overview

Many groups have characterized aspects of Mars' south polar cap, and various naming schemes for different units have been developed [Tanaka *et al.*, 2007; Thomas *et al.*, 2013; Phillips *et al.*, 2011]. This paper will use a naming scheme modified from that of Tanaka *et al.* [2007] and given in Table 1. The compositional

Table 1. Stratigraphic Units in the Australe Mensa Region of the SPLD^a

Group Names	Unit Name	Ice Composition	Unit Thickness (m)
SPRC	A _{A4b}	CO ₂	10 ^b
	AA _{4a}	H ₂ O	
RFZ ₃	BL ₃	H ₂ O	< 20
	AA _{3c}	CO ₂	300
	BL ₂	H ₂ O	40
	AA _{3b}	CO ₂	< 700
	BL ₁	H ₂ O	20
	AA _{3a}	CO ₂	200
	AA ₂	H ₂ O	300 ^c
	AA ₁	H ₂ O	3500 ^c

^aUnits are ordered with the surface at the top. Methods used to determine ice compositions and thickness in RFZ₃ are presented in sections 2 and 3. Note that the geologic unit AA₃ is not subdivided in *Tanaka et al.* [2007].

^b*Thomas et al.* [2005] and *Tanaka et al.* [2007].

^c*Kolb et al.* [2006].

labels assigned to each unit are justified in sections 2 and 3. The radar unit RFZ₃ [Phillips *et al.*, 2011] and observationally mapped unit AA₃ will be used interchangeably as justified in section 2.

With an enhanced radar mapping effort, we show that the RFZ₃ unit is more extensive and locally deeper than originally mapped. We find three distinct CO₂ subunits, each capped by a bounding layer (BL). We use a combination of radar and surface observations to constrain the composition of the observed subunits. We propose a scenario in which CO₂ ice is deposited over much of the poles during low obliquity periods. This ice subsequently retreats until a remnant is sequestered below a water ice deposit (BL subunits), removing it from contact with the atmosphere.

2. Radar Observations

Phillips *et al.* [2011] mapped four reflection-free zones (RFZs) within the SPLD. Based on estimates of permittivity, the most poleward of those zones, RFZ₃, was shown to be massive CO₂ ice with a volume of ~4500 km³. This volume incorporated locations where RFZ₃ was easily detected with SHARAD but excluded the region poleward of 87°S, where there is no radar coverage due to the orbital inclination of MRO. Their analysis included observations from 129 orbital passes, and the coverage was too sparse to find the northern boundary of the deposits or completely fill gaps. They demonstrated a reasonable but imperfect correlation of RFZ₃ with the image-based geologic unit AA₃ [Kolb *et al.*, 2006; Tanaka *et al.*, 2007; Phillips *et al.*, 2011]. To provide a better estimate of the total volume of RFZ₃, the measured unit was extrapolated to coincide with the boundaries of AA₃ as mapped in optical imagery.

Here we improve upon the prior study by including an additional 300 radar observations that cover a larger area and fill gaps in the previous coverage. With this new mapping effort, detections of RFZ₃ correspond to the northern bounds of the optically imaged AA₃ (Figure 1). We also find the unit in two previously unmapped areas and include a portion of AA₃ omitted from the previous study (red arrows in Figure 1). This improvement in correlation between AA₃ and RFZ₃ carries a twofold importance. First, it provides confidence in using AA₃ to extrapolate the extent of RFZ₃ poleward of 87°S. Second, it strengthens the case for interpretations of RFZ₃ as a CO₂ deposit based on optically imaged sublimation troughs and pits that are unique to AA₃. No other unit on the water ice dominated SPLD exhibits these features [Phillips *et al.*, 2011].

Further improvements are provided by better detection of the RFZ₃ base (Figure 2). At the most southerly latitudes observed by SHARAD, our mapping yields maximum depths of just over 1000 m (blue arrow in Figure 1), whereas ~700 m was the previously reported maximum. Better spatial coverage and enhanced radar processing have improved confidence in the placement of this lower boundary.

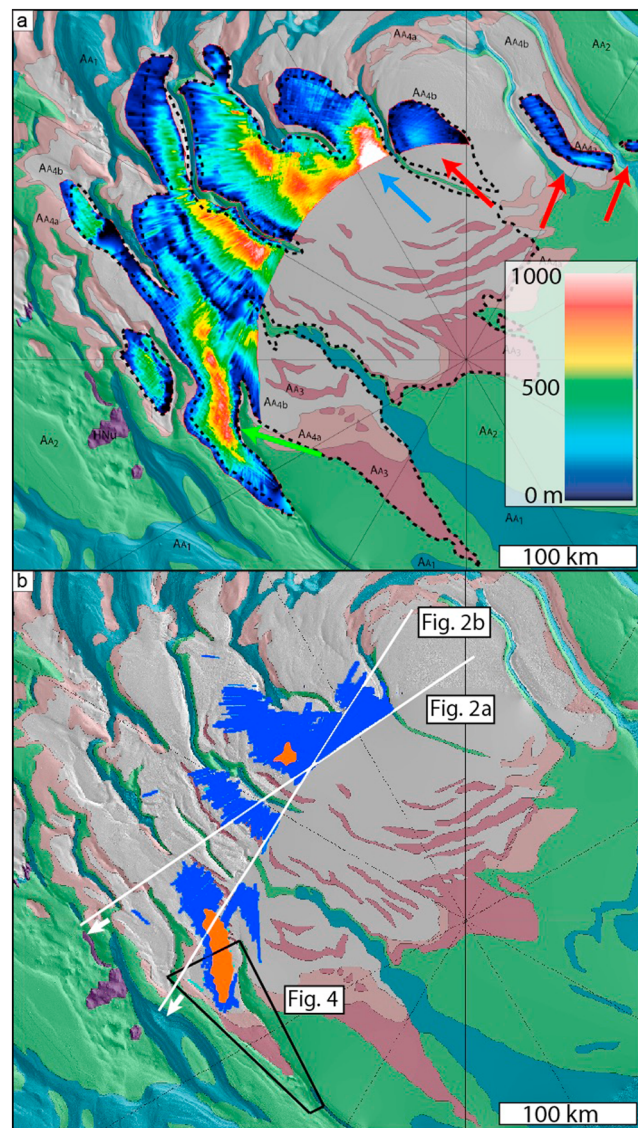


Figure 1. (a) Maximum depth map of RFZ₃ deposits and (b) extent of the bounding layers. In Figure 1b BL₁ is mapped as orange and BL₂ is mapped in blue. Base geologic map is from Tanaka *et al.* [2007]. Red arrows indicate areas not mapped by Phillips *et al.* [2011]. The location of the thickest (>1000 m) part of RFZ₃ mapped is indicated by the blue arrow. The green arrow points to a location that was found to be thicker than was estimated in Phillips *et al.* [2011] due to the presence of a deeper bounding layer 1 (BL₁).

Another enhancement of our depth measurements is found at lower elevations. In addition to the original bounding layer (BL₂) that separates two CO₂ subunits of RFZ₃ in many locations, we find a second bounding layer (BL₁) (Figure 2). Where it is present, BL₁ was previously interpreted to be the base of RFZ₃. The inclusion of the third subunit increases the measured depth of the RFZ₃ base in this location by as much as 300 m (green arrow in Figure 1).

BL₁ and BL₂ are not exposed on the surface, so constraints on their material properties are limited to radar measurements. The strong reflection produced at the boundaries requires that the BLs must have permittivity distinct from the surrounding CO₂. Volumetrically, the only viable candidate material is water ice. This water ice may, however, have some dust and CO₂ (as a clathrate hydrate) incorporated into it [Jakosky *et al.*, 1995]. Using a forward model (section S1), we find the concentration of such contaminants must be low. When considering a permittivity characteristic of water ice (3.15) the bounding layers vary in thickness from less than the resolution limit of SHARAD (~11 m in water ice) to 64 m with a mean of 37 m.

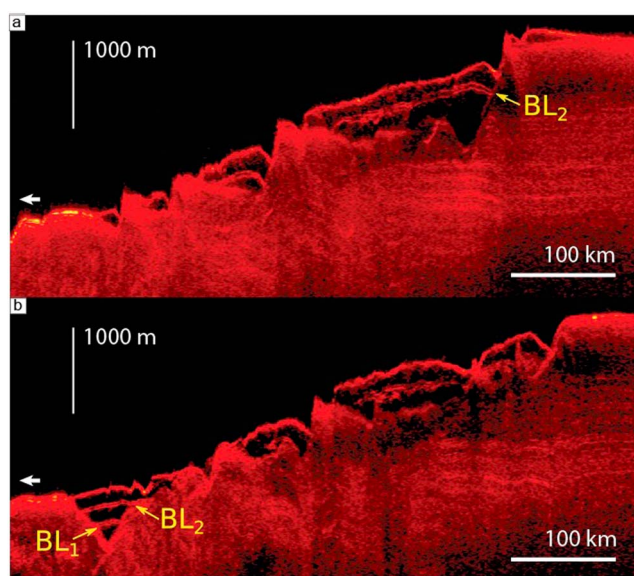


Figure 2. SHARAD observations (a) 2326801 and (b) 724802. The ground tracks of these observations are shown in Figure 1b. Note the occurrence of two bounding layers in the low-reflectivity zone on the left side of Figure 2b. Radargrams are converted to depth assuming CO₂ ice (dielectric of 2.1) in RFZ₃ and water ice (dielectric of 3.15) elsewhere in the subsurface.

The expanded SHARAD coverage and the newly measured depths add to the measured volume of RFZ₃, which has increased from 4500 km³ to 7700 km³ prior to extrapolation (Figure 1a). We extrapolate poleward bounded by the optically imaged extent of AA₃ using a natural neighbor method and obtain a new volume of 14,800 km³ for RFZ₃, 18% greater than that of Phillips *et al.* [2011]. We assume zero porosity and no contaminants, so the density of RFZ₃ is that of CO₂ ice, ~1600 kg/m³ [Piqueux *et al.*, 2003], and the total mass of this unit is then 2.4×10^{16} kg, essentially equal to the mass of the Martian atmosphere (2.5×10^{16} kg) [James and North, 1982]. If totally sublimated, this mass would increase the current average surface pressure by 610 Pa, doubling the present value and enhancing the stability of liquid water at the surface.

3. Surface Observations

Figure 3 presents a stretched CTX image of a part of the SPLD containing the SPRC CO₂ and H₂O (AA_{4a} and AA_{4b}) subunits. Both are bright, but the CO₂ has a mottled appearance due to the "Swiss cheese" sublimation features [Thomas *et al.*, 2005]. The unit AA₃ is darker and uniquely contains troughs (not shown) that exhibit a mixture of dust, water ice, and dry ice, as measured by the OMEGA instrument in late summer [Douté *et al.*, 2007]. Thus, spectral measurements do not provide compelling evidence for or against a water ice cap over RFZ₃ (BL₃). However, a polygonal pattern (Figure 3b) at the surface of AA₃ with a characteristic dimension of about 20 m is found on no other unit in the SPLD. These polygons are highly distinct from the CO₂ sublimation features on the SPRC and most closely resemble polygonal features seen in other thermally stressed water ice deposits on Mars [Mellon *et al.*, 2008]. Thus, we propose that the polygons are unique to AA₃ because it is the only region in the SPLD where dry ice lies beneath a relatively thin layer of water ice. Given this, the observed polygonal terrain could be caused by stresses initiated by the fact that the coefficient of thermal expansion of CO₂ ice [Manzhelii *et al.*, 1971] is an order of magnitude larger than that for water ice [Röttger *et al.*, 1994]. If BL₃ is 20 m thick SHARAD would resolve a basal reflection (which it does not), and the thermal stress would decrease by about a factor of 2.5. Therefore, BL₃ must be thinner than BL₂ on average.

If both BL₃ and AA_{4a} are water ice layers, it raises a question of why they are so distinct in observations. Figure 3 shows that BL₃ is noticeably darker than AA_{4a} and only BL₃ shows the polygonal terrain. One hypothesis is that these layers were deposited with different dust fractions. Alternatively, BL₃ may have formed with the same initial dust fraction as AA_{4b} and subsequent sublimation of BL₃ produced a dark lag deposit at the surface. Both scenarios require two periods of water ice deposition. Modeling by Montmessin *et al.* [2007] suggests the last period of water ice deposition at the south polar cap was ~20 kyr ago with their largest uncertainty being how dust cycles change with orbital parameters. Future modeling efforts should investigate if variable dust loading or other factors could cause the difference observed in these two units.

4. Modeling CO₂ Ice Accumulation

To model the depositional history of CO₂ ice at the poles, we followed the methods of Manning *et al.* [2006] and Wood *et al.* [2012], who performed seasonally resolved calculations of the evolution of Mars' atmospheric pressure and polar CO₂ deposits from 800 kyr to the present. This zonally symmetric model includes subsurface

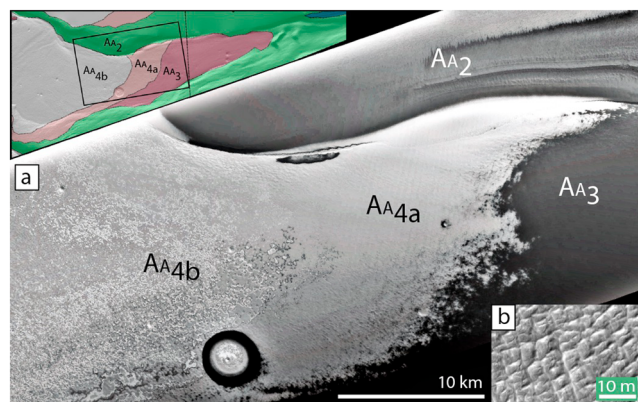


Figure 3. (a) Stretched CTX image P10_005036_0870_XI_875114W which shows the surface expression of the different units in the SPLD. High Resolution Imaging Science Experiment (HIRISE) image PSP_005349_0930 shows the AA₃ shows regular polygons of order 20 m. This HIRISE section is from the sublimation pit in the lower part of Figure 3a.

heat conduction, insolation-dependent albedo [Guo *et al.*, 2010], and Mars orbital variations [Laskar *et al.*, 2004]. In its base setup this model has surface CO₂ in constant contact with the atmosphere. For more details on the model, see Wood *et al.* [2012] and supporting information.

Our model predicts that the SPLD has experienced five periods of CO₂ accumulation up to 150 m at 89°S during the last 800 kyr (Figures 4 and S4). Each period of CO₂ ice deposition corresponds to the removal of a few hundred pascals from the atmosphere (Figure 4). Our base model does not sequester the ice, and it returns to the atmosphere at the end of each period of high obliquity (Figure S4). However, the presence of the RFZ₃ unit

requires some mechanism to stabilize and protect the deposit in periods of high obliquity. Given the evidence of water ice bounding layers (see previous section), it is natural to assume that water ice stabilizes each RFZ₃ subunit during periods of high obliquity.

The amount of water ice needed to thermally protect an underlying CO₂ deposit can be estimated by comparing the CO₂ phase curve with an estimate of the annual thermal wave. Assuming a single-mode thermal wave [Turcotte and Schubert, 2014], we calculate the maximum temperature at a given depth (T_{\max}) as

$$T_{\max} = T_{\text{mean}} + \Delta T \exp(-z/d_{\omega}), \quad (1)$$

where T_{mean} is the mean annual surface temperature, ΔT is the annual temperature anomaly, z is the depth below the surface, and d_{ω} is the annual thermal skin depth. This single-mode assumption does not capture the fact that during the winter the surface temperatures are being fixed at the sublimation temperature of CO₂. To try and offset this effect, we over estimate ΔT . Our modeled results indicate that approximately 10 m of water ice is enough to stabilize the CO₂ ice even with a large thermal wave (Figure S2). This result is consistent with previous work by Jakosky *et al.* [1995]. The thickness of a water ice layer needed to stabilize the underlying CO₂ is not very sensitive to ΔT because of the exponential decay of the thermal wave with depth. It is, however, very sensitive to T_{mean} , which is itself a function of obliquity. Taken at face value, this model implies that 37 m of H₂O ice could stabilize the underlying CO₂ ice up to a mean annual temperature of ~190 K. Even at large obliquity, T_{mean} is not expected to rise above ~180 K [Jakosky *et al.*, 1995]. This implies that the stability of the AA₃ subunits is controlled by the stability of the water ice BL's capping them.

This optimistic preservation model assumes that the CO₂ is under lithostatic pressure and thus requires that no cracks penetrate through the overlying water ice. This assumption is validated by the fact that CO₂ sublimation pits in AA₃ are rare unless they are associated with troughs, where they are plentiful [Phillips *et al.*, 2011]. We attribute this association to the local relief of lithostatic pressure in the troughs.

To estimate a minimum age for AA₃, we incorporate the insulating effect of the BLs during periods of high obliquity. This is done by removing the CO₂ ice from contact with the atmosphere in some climate model runs, effectively sequestering it over several obliquity cycles. This step allows the model to predict the evolution of surface pressure and total thickness of the CO₂ ice deposits integrated over 380 kyr (Figures 4 and S5). These simulations reveal that during certain periods, the surface pressure regularly drops below the current value of 610 Pa and that its long-term equilibrium value is ~1250 Pa. Annual variability in surface pressure may range from 1100 Pa to 1350 Pa during these periods (Figure S4).

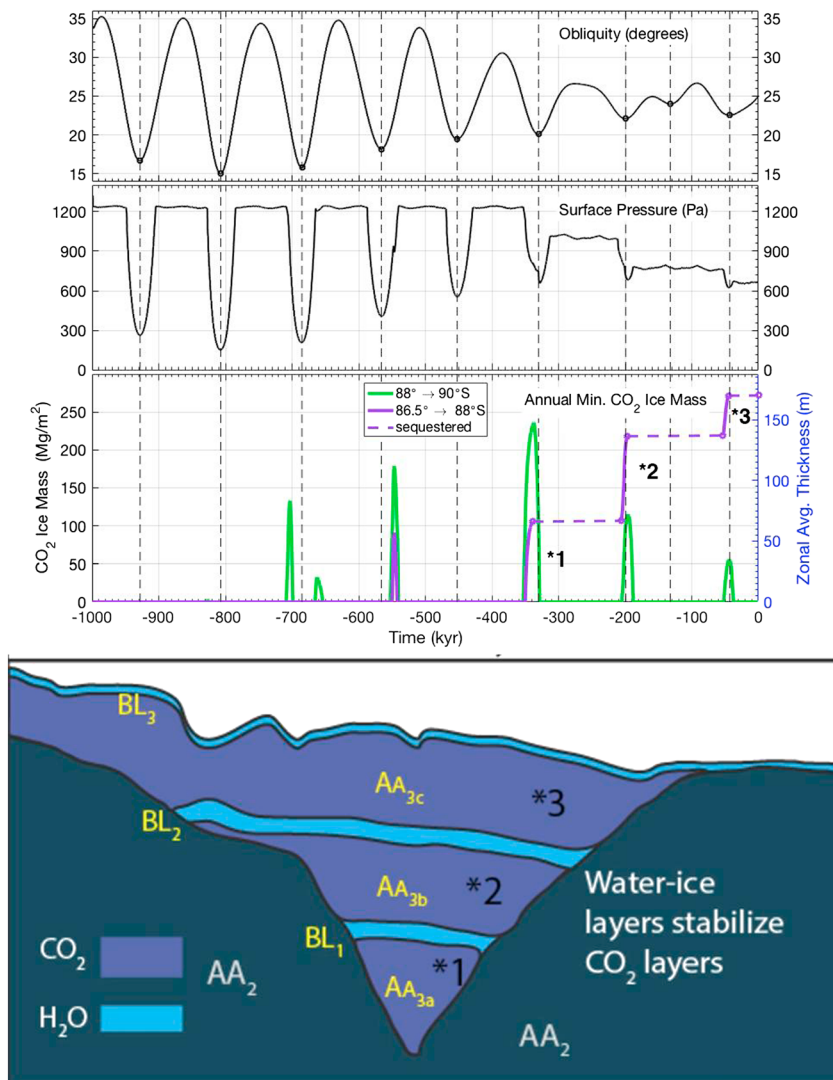


Figure 4. (top) Results from our stability model using 400 kg/m² global CO₂ budget (consistent with total budget of $\sim 5.8 \times 10^{16}$ kg). Obliquity from *Laskar et al.* [2004] is shown in the top black line for reference. Vertical dashed lines are minimums in obliquity. The green and purple lines track the regional average CO₂ ice thickness over several obliquity cycles. In this base model run CO₂ ice is not preserved between obliquity cycles. The dashed purple line does the same, with the deposited CO₂ removed from contact with the atmosphere to mimic the effect of an insulating cap layer over the CO₂. (middle) Pressure variations for the latter case. The time offset between minimum surface pressures and maximum ice thickness is due to other CO₂ deposits at the north pole (shown in Figure S3). (bottom) A cartoon profile of how the observed bounding layer stratigraphy (also shown in Figure 2b) may correspond to the last three modeled obliquity cycles. This proposed history of the AA₃ deposit represents the minimum possible age, as older units may have been preserved in place of younger ones.

5. Discussion

Our improved mapping of RFZ₃ and modeling work presented above provide a framework to understand the history of CO₂ reserves on Mars. Previous studies had shown that large quantities of CO₂ can be deposited on the polar cap during times of low obliquity [*Armstrong et al.*, 2004; *Manning et al.*, 2006; *Wood et al.*, 2012]; however, those studies (with the exception of *Wood et al.* [2012]) underestimated the CO₂ budget of the planet because they did not incorporate the full quantity of CO₂ presently sequestered in the SPLD. Furthermore, those studies did not include mechanisms by which the deposits might persist between periods of low obliquity.

The radar data shows that the ice distribution is not symmetric about the pole but is longitudinally bound between $\sim 240^\circ$ and $\sim 360^\circ$ E, a pattern that is also consistent with the residual CO₂ cap. There are three,

nonexclusive, mechanisms that might explain this distribution, a bias in preservation: a bias in accumulation, or lateral movement. The area where the CO₂ resides is a local minimum in the topography. This could cause a preservation bias if it allows the overlying water ice to more easily remove the CO₂ from contact with the atmosphere. Lower altitudes are also favored for CO₂ deposition because of the higher atmospheric pressure [Kreslavsky and Head, 2005]. Global circulation models have demonstrated the Hellas and Argyre basins have pronounced effects on where CO₂ ice is deposited [Colaprete et al., 2005] and similar forcing may have been present for the deposition of AA₃. Lastly, there is some literature discussing the geologic evidence for CO₂ glaciers on Mars [Kreslavsky and Head, 2011]. While evidence for CO₂ glaciers has not been observed in the Southern hemisphere [Kreslavsky and Head, 2011], we cannot rule out the possibility that the areal distribution of CO₂ has been affected by glacial flow. Future work should examine each of these possibilities in more detail to better understand the history of Martian CO₂ transport.

We find evidence of two bounding layers between the CO₂ subunits of RFZ₃ suggesting that the CO₂ ice was emplaced during three periods. A bounding layer caps each RFZ₃ subunit and protects it during periods of high obliquity. Our measurements of the dielectric properties of the bounding layers are consistent with nearly pure water ice between 15 and 60 m thick. Modeling described in section 4 finds that these thicknesses are sufficient for reducing the sublimation rate of CO₂ ice to near-zero values.

This opens the question of what controls the change from CO₂ deposition to water ice deposition. *Montmessin et al.* [2007] have suggested that in the recent past, changes in the longitude of perihelion may control which polar cap is favorable for water ice deposition. The thickness of the BLs could be accumulated in tens of thousands of years at the deposition rates suggested by *Montmessin et al.* [2007]. The longitude of perihelion changes much faster than obliquity, with a period of about 50 kyr [Laskar et al., 2004]. While the details should be studied carefully by future work, it is at least plausible that these changing orbital parameters could switch between regimes of CO₂ deposition to water ice deposition.

Our model predicts that during the last 1000 kyr, four periods of perennial CO₂ ice deposition left thick, extensive CO₂ deposits at observed RFZ latitudes (84°S–87°S). We suggest that during subsequent sublimation, three of those deposits were preserved in topographic depressions by water ice layers, effectively halting the loss of CO₂ reserves into the atmosphere. Each time, the atmospheric pressure returned to lower values than the long-term equilibrium. During the periods of greatest collapse (which occurred on both poles), the surface pressure may fall to values as low as 200 Pa, about a third of the present-day value. These periods profoundly impede the mobility of dust, sand, and volatiles. The water ice polar caps, covered by CO₂ ice, may be cut off entirely from the atmosphere, reducing volatile availability via another mechanism. Finally, at the highest pressures expected during this period, 1350 Pa, liquid water would be stable at many more locations than at present, and dunes that appear inactive in the current climate could become active, explaining the divergent orientations of many dunes relative to current wind regimes [Ewing et al., 2010]. This proposed history provides the minimum possible age of the AA₃ deposit, ~300 kyr for the oldest units. It is possible that older units may have been preserved in place of younger ones, a question that should be explored by future models of CO₂ and water ice stability on obliquity timescales.

Acknowledgments

Data used in this work are available from the NASA Planetary Data System or from the Colorado SHARAD Processing System (CO-SHARPS). E-mail co-sharps@spaceops.swri.org for more information. The authors thank the two anonymous reviewers for their feedback.

References

- Armstrong, J. C., C. B. Leovy, and T. Quinn (2004), A 1 Gyr climate model for Mars: New orbital statistics and the importance of seasonally resolved polar processes, *Icarus*, 171(2), 255–271, doi:10.1016/j.icarus.2004.05.007.
- Becerra, P., S. Byrne, and A. J. Brown (2015), Transient bright “halos” on the south polar residual cap of Mars: Implications for mass-balance, *Icarus*, 251, 211–225, doi:10.1016/j.icarus.2014.04.050, dynamic Mars.
- Byrne, S., P. Hayne, P. Becerra, and H. Team (2014), Evolution and stability of the residual CO₂ ice cap, paper presented at Eighth International Conference on Mars, p.1252, LPI Contribution No. 1791, Pasadena, Calif., 14–18 Jul.
- Colaprete, A., J. R. Barnes, R. M. Haberle, J. L. Hollingsworth, H. H. Kieffer, and T. N. Titus (2005), Albedo of the South Pole on Mars determined by topographic forcing of atmosphere dynamics, *Nature*, 435(7039), 184–188.
- Douté, S., B. Schmitt, Y. Langevin, J.-P. Bibring, F. Altieri, G. Bellucci, B. Gondet, and F. Poulet (2007), South pole of Mars: Nature and composition of the icy terrains from Mars express omega observations, *Planet. Space Sci.*, 55(1–2), 113–133, doi:10.1016/j.pss.2006.05.035.
- Ewing, R. C., A.-P. B. Peyret, G. Kocurek, and M. Bourke (2010), Dune field pattern formation and recent transporting winds in the Olympia Undae Dune Field, north polar region of Mars, *J. Geophys. Res.*, 115, E08005, doi:10.1029/2009JE003526.
- Forget, F. (1998), Mars CO₂ ice polar caps, in *Solar System Ices*, pp. 477–507, Springer, Dordrecht, Netherlands.
- François, L. M., J. C. G. Walker, and W. R. Kuhn (1990), A numerical simulation of climate changes during the obliquity cycle on Mars, *J. Geophys. Res.*, 95(B9), 14,761–14,778, doi:10.1029/JB095iB09p14761.
- Guo, X., M. I. Richardson, A. Soto, and A. Toigo (2010), On the mystery of the perennial carbon dioxide cap at the south pole of Mars, *J. Geophys. Res.*, 115, E04005, doi:10.1029/2009JE003382.
- Head, J. W., J. F. Mustard, M. A. Kreslavsky, R. E. Milliken, and D. R. Marchant (2003), Recent ice ages on Mars, *Nature*, 426(6968), 797–802, doi:10.1038/nature02114.

- Hess, S., J. Ryan, J. Tillman, R. Henry, and C. Leovy (1980), The annual cycle of pressure on Mars measured by Viking Landers 1 and 2, *Geophys. Res. Lett.*, *7*(3), 197–200, doi:10.1029/GL007i003p00197.
- Hess, S. L., R. M. Henry, and J. E. Tillman (1979), The seasonal variation of atmospheric pressure on Mars as affected by the south polar cap, *J. Geophys. Res.*, *84*(B6), 2923–2927, doi:10.1029/JB084iB06p02923.
- Jakosky, B. M., B. G. Henderson, and M. T. Mellon (1995), Chaotic obliquity and the nature of the Martian climate, *J. Geophys. Res.*, *100*(E1), 1579–1584, doi:10.1029/94JE02801.
- James, P. B., and G. R. North (1982), The seasonal CO₂ cycle on Mars: An application of an energy balance climate model, *J. Geophys. Res.*, *87*(B12), 10,271–10,283, doi:10.1029/JB087iB12p10271.
- Kolb, E., K. Tanaka, R. Greeley, G. Neukum, and the HRSC Co-Investigator Team (2006), The residual ice cap of Planum Australe, Mars: New insights from the HRSC experiment, paper presented at Lunar and Planetary Science Conference, Lunar and Planetary Institute, Houston, Tex.
- Kreslavsky, M., and J. Head (2002), Mars: Nature and evolution of young latitude-dependent water-ice-rich mantle, *Geophys. Res. Lett.*, *29*(15), 1719, doi:10.1029/2002GL015392.
- Kreslavsky, M. A., and J. W. Head (2005), Mars at very low obliquity: Atmospheric collapse and the fate of volatiles, *Geophys. Res. Lett.*, *32*, L12202, doi:10.1029/2005GL022645.
- Kreslavsky, M. A., and J. W. Head (2011), Carbon dioxide glaciers on Mars: Products of recent low obliquity epochs (?), *Icarus*, *216*(1), 111–115, doi:10.1016/j.icarus.2011.08.020.
- Laskar, J., B. Levrard, and J. F. Mustard (2002), Orbital forcing of the Martian polar layered deposits, *Nature*, *419*(6905), 375–377, doi:10.1038/nature01066.
- Laskar, J., A. C. M. Correia, M. Gastineau, F. Joutel, B. Levrard, and P. Robutel (2004), Long term evolution and chaotic diffusion of the insolation quantities of Mars, *Icarus*, *170*(2), 343–364, doi:10.1016/j.icarus.2004.04.005.
- Levrard, B., F. Forget, F. Montmessin, and J. Laskar (2007), Recent formation and evolution of northern Martian polar layered deposits as inferred from a global climate model, *J. Geophys. Res.*, *112*, E06012, doi:10.1029/2006JE002772.
- Madeleine, J.-B., F. Forget, J. W. Head, B. Levrard, F. Montmessin, and E. Millour (2009), Amazonian northern mid-latitude glaciation on Mars: A proposed climate scenario, *Icarus*, *203*(2), 390–405, doi:10.1016/j.icarus.2009.04.037.
- Manning, C., C. McKay, and K. Zahnle (2006), Thick and thin models of the evolution of carbon dioxide on Mars, *Icarus*, *180*(1), 38–59, doi:10.1016/j.icarus.2005.08.014.
- Manzhelii, V. G., A. M. Tolkahev, M. I. Bagatskii, and E. I. Voitovich (1971), Thermal expansion, heat capacity, and compressibility of solid CO₂, *Phys. Status Solidi B*, *44*(1), 39–49, doi:10.1002/pssb.2220440104.
- Mellon, M. T., R. E. Arvidson, J. J. Marlow, R. J. Phillips, and E. Asphaug (2008), Periglacial landforms at the Phoenix landing site and the northern plains of Mars, *J. Geophys. Res.*, *113*, E00A23, doi:10.1029/2007JE003039.
- Montmessin, F., R. M. Haberle, F. Forget, Y. Langevin, R. T. Clancy, and J.-P. Bibring (2007), On the origin of perennial water ice at the south pole of Mars: A precession-controlled mechanism?, *J. Geophys. Res.*, *112*, E08S17, doi:10.1029/2007JE002902.
- Murray, B. C., W. R. Ward, and S. C. Yeung (1973), Periodic insolation variations on Mars, *Science*, *180*(4086), 638–640.
- Phillips, R. J., et al. (2011), Massive CO₂ ice deposits sequestered in the south polar layered deposits of Mars, *Science*, *332*(6031), 838–41, doi:10.1126/science.1203091.
- Piqueux, S., S. Byrne, and M. I. Richardson (2003), Sublimation of Mars's southern seasonal CO₂ ice cap and the formation of spiders, *J. Geophys. Res.*, *108*(E8), 5084, doi:10.1029/2002JE002007.
- Röttger, K., A. Endriss, J. Ihringer, S. Doyle, and W. F. Kuhs (1994), Lattice constants and thermal expansion of H₂O and D₂O ice Ih between 10 and 265 K, *Acta Crystallogr. Sec. B*, *50*(6), 644–648, doi:10.1107/S0108768194004933.
- Seu, R., et al. (2007), Sharad sounding radar on the Mars Reconnaissance Orbiter, *J. Geophys. Res.*, *112*, E05S05, doi:10.1029/2006JE002745.
- Tanaka, K., E. Kolb, and C. Fortezzo (2007), Recent advances in the stratigraphy of the polar regions of Mars, *LPI Contributions*, 3–6, The Seventh International Conference on Mars, Pasadena, Calif., 7–13 Jul.
- Thomas, P., M. Malin, P. James, B. Cantor, R. Williams, and P. Gierasch (2005), South polar residual cap of Mars: Features, stratigraphy, and changes, *Icarus*, *174*(2), 535–559, doi:10.1016/j.icarus.2004.07.028, Mars Polar Science III.
- Thomas, P., W. Calvin, P. Gierasch, R. Haberle, P. James, and S. Sholes (2013), Time scales of erosion and deposition recorded in the residual south polar cap of Mars, *Icarus*, *225*(2), 923–932, doi:10.1016/j.icarus.2012.08.038.
- Thomas, P., W. Calvin, B. Cantor, R. Haberle, P. James, and S. Lee (2016), Mass balance of Mars' residual south polar cap from CTX images and other data, *Icarus*, *268*, 118–130, doi:10.1016/j.icarus.2015.12.038.
- Tillman, J. E., N. C. Johnson, P. Guttorp, and D. B. Percival (1993), The Martian annual atmospheric pressure cycle: Years without great dust storms, *J. Geophys. Res.*, *98*(E6), 10,963–10,971, doi:10.1029/93JE01084.
- Toon, O. B., J. B. Pollack, W. Ward, J. A. Burns, and K. Bilski (1980), The astronomical theory of climatic change on Mars, *Icarus*, *44*(3), 552–607.
- Turcotte, D. L., and G. Schubert (2014), *Geodynamics*, Cambridge Univ. Press, New York.
- Ward, W. R. (1973), Large-scale variations in the obliquity of Mars, *Science*, *181*(4096), 260–262.
- Ward, W. R. (1974), Climatic variations on Mars: 1. Astronomical theory of insolation, *J. Geophys. Res.*, *79*(24), 3375–3386.
- Ward, W. R., B. C. Murray, and M. C. Malin (1974), Climatic variations on Mars: 2. Evolution of carbon dioxide atmosphere and polar caps, *J. Geophys. Res.*, *79*(24), 3387–3395.
- Wood, S. E., S. D. Griffiths, and J. Bapst (2012), Mars at low obliquity: Perennial CO₂ caps, atmospheric collapse, and subsurface warming, paper presented at Eighth International Conference on Mars, LPI Contribution No. 1791, Pasadena, Calif., 14–18 Jul.